compounds

MDPI

Article

The Role of Zinc Oxide as a Resistivity Modulator in Complex Polymer Compounds for Cable Application

Stefano Dossi [1], Pietro Matteucci [1], Andrea Galanti [1], Flavia Bartoli [2,*], Sabrina Bianchi [2] and Francesco Ciardelli [2,3]

[1] Mixer S.p.A., Via Chiara n. 6/C, 48012 Villa Prati di Bagnacavallo, RA, Italy; sdossi@mixercompounds.com (S.D.); pmatteucci@mixercompounds.com (P.M.); agalanti@mixercompounds.com (A.G.)
[2] SPINPET S.r.l., Viale R. Piaggio 32, 56025 Pontedera, PI, Italy; bianchi@spinpet.it (S.B.); francesco.ciardelli@unipi.it (F.C.)
[3] Department of Chemistry and Industrial Chemistry, University of Pisa, Via Giuseppe Moruzzi 13, 56124 Pisa, PI, Italy
* Correspondence: bartoli@spinpet.it; Tel.: +39-0587274832

Abstract

For cable compound manufacturers, accurate formulation fine-tuning is essential to ensure safety, long-term durability, and compliance with international standards for dielectric strength, volume resistivity, and environmental and thermal ageing. This work presents an experimental study demonstrating how minor additives can critically affect the performance of complex flame-retardant elastomeric formulations. The investigation focuses on the role of small amounts of zinc oxide (ZnO) in commercial cable compounds based on a crosslinked elastomeric matrix composed of ethylene–propylene monomer (EPM), ethylene–propylene–diene monomer (EPDM), and thermoplastic polyolefin elastomer (POE). The formulations contain aluminium trihydroxide (ATH) as the major filler, together with several minor additives. Among these, a phenolic antioxidant (AN01) acting as a metal deactivator is also present. The addition of ZnO in low amounts (2–5 phr) allowed the compounds to maintain a volume resistivity $\geq 10^{12}$ Ω·cm in water at 100 °C. To elucidate the role of ZnO, a systematic set of formulations was prepared by varying the type and content of selected additives. The compounds were prepared by melt mixing in an internal mixer (Banbury type), followed by peroxide crosslinking via compression molding. Electrical characterization results indicate that ZnO interacts with the phenolic additive through surface adsorption, forming a coated particle with significantly reduced electrical conductivity. Optimal electrical performance was achieved when the ZnO-to-additive ratio corresponded to the minimum amount required for complete surface complexation.

Keywords: elastomeric cable compounds; flame-retardant materials; electrical volume resistivity; zinc oxide additives; formulation fine-tuning

Check for updates

Academic Editor: Gabriel A. Lopez

Received: 11 March 2026
Revised: 13 April 2026
Accepted: 21 April 2026
Published: 24 April 2026

Copyright: © 2026 by the authors. Licensee MDPI, Basel, Switzerland. This article is an open access article distributed under the terms and conditions of the Creative Commons Attribution (CC BY) license.

1. Introduction

Peroxide-curable elastomeric insulation compounds are widely used in low-, medium-, and high-voltage cable systems, where long-term electrical stability under thermal and environmental stress is essential [1–3]. These materials are employed in power distribution, automotive and e-mobility wiring, renewable-energy installations, and industrial control cables, all requiring insulation capable of maintaining high resistivity and dielectric strength over extended service life. In low-voltage applications ($\leq$1 kV), such as building wiring and

automotive harnesses, insulation must combine thermal ratings up to 90–125 °C, flexibility, and stable electrical performance during overloads [1]. Medium-voltage systems (1–35 kV), including distribution grids and renewable interconnections, impose stricter requirements, such as resistance to higher electric fields, thermal cycling, moisture ingress, and partial discharges [2,3]. At high voltage (>35 kV), materials must ensure high dielectric purity and resistance to thermo-oxidative degradation to prevent premature breakdown [1–3]. To meet these demands, cable manufacturers employ elastomers such as EPDM, EVA, EPR, silicone rubber (VMQ), and polyolefin-based elastomers [1,2]. Among these, peroxide-curable systems are preferred because peroxide crosslinking forms a stable three-dimensional network, enhancing heat resistance, elasticity, and retention of electrical properties compared to sulfur-cured systems [4,5]. Moreover, peroxide curing avoids ionic residues and metal-containing accelerators typical of sulfur systems, which can increase dielectric losses and reduce volume resistivity [4].

These advantages make peroxide-crosslinked elastomers suitable for applications requiring high thermal endurance, low dielectric loss, and high-volume resistivity (ρ_V). However, dielectric strength can decrease under thermal stress, and ρ_V is particularly sensitive to temperature and moisture, which can significantly reduce insulating performance [6–9]. A key challenge is therefore the development of materials combining flame-retardant performance with stable electrical behavior under harsh service conditions. This requires careful optimization of both fillers and minor additives, whose interactions become particularly critical in peroxide-crosslinked systems [1,2].

Among the additives commonly used in elastomeric insulation compounds, ZnO is of particular interest. It is a semiconducting oxide with a direct band gap of 3.4 eV and a dielectric constant of about 8.5–9.5 [10]. ZnO is widely employed to modify mechanical, optical, and electrical properties, and in elastomers it can improve processability, ageing resistance, and crosslinking behavior [10]. ZnO is also known to develop high-resistivity surface layers (Schottky-type barriers) due to oxygen adsorption, which can strongly influence charge transport at interfaces and in highly filled systems [11,12]. Numerous studies have investigated ZnO in relatively simple polymer matrices, particularly polyolefins, where it affects dielectric and varistor-like behavior [5,12–15]. However, much less attention has been devoted to ZnO in complex, industry-relevant formulations containing multiple interacting additives and high filler loadings. In such systems, the coexistence of metal oxides, hydroxide flame retardants, antioxidants, metal deactivators, coagents, and processing aids creates a multicomponent environment in which ZnO behavior may differ significantly from that observed in simplified systems. This is particularly relevant under cable qualification conditions, which involve prolonged exposure to hot water, elevated temperature, and electrical stress. Under these conditions, water can penetrate the polymer–filler interface and influence additive mobility, dissociation equilibria, and interfacial polarization, ultimately affecting electrical resistivity [15–17].

Industrial experience with peroxide-cured, highly filled elastomeric systems has shown that exposure to hot water can lead to unexpected decreases in ρ_V, even when dry-state properties meet specifications. In several cases, the addition of small amounts of ZnO mitigates this loss of performance. Although these effects are well known in practice, their molecular origin remains unclear, particularly regarding the interactions between ZnO and specific additives under hot–wet conditions.

Further complexity arises from interactions among minor additives. Additives rarely act independently; the combination thereof may produce synergistic or antagonistic effects [18,19]. Such interactions have been widely reported in polyolefins, for example between HALS and phenolic antioxidants or thiosynergists, significantly affecting long-term stability [18,19]. In highly filled elastomeric systems, the coexistence of fillers, flame

retardants, antioxidants, coagents, and functional additives creates a complex interaction network involving surface chemistry, additive mobility, and competitive adsorption. In particular, ZnO has been shown to adsorb hindered phenolic antioxidants (e.g., Irganox 1076) from polyethylene, reducing oxidative stability; moreover, uncoated ZnO nanoparticles containing ionic species can promote radical formation [20]. In peroxide-crosslinked systems, adsorption of crosslinking by-products such as acetophenone and cumyl alcohol, together with antioxidant depletion, may further modify the local chemical environment and influence electrical performance [20]. Understanding these interactions is therefore essential for rational formulation design and for predicting long-term behavior under service conditions. Although extensive literature exists on ZnO in simplified systems, its applicability to complex, highly filled formulations remains limited.

Accordingly, this work aims to clarify the mechanism by which ZnO influences electrical resistivity in complex elastomeric compounds under hot–wet conditions, and to identify the formulation components most strongly interacting with ZnO. A stepwise experimental approach was adopted to separate the contributions of individual components from those of the full formulation. First, simplified model compounds were prepared by removing minor additives to isolate the intrinsic effect of ZnO in ATH- or kaolin-filled matrices. Then, selected additives and their combinations were progressively reintroduced to identify the most relevant interactions. Finally, systems with fixed metal deactivator (MD) content and varying ZnO concentrations were prepared to investigate the role of the ZnO/MD ratio on resistivity under hot–wet conditions.

This approach provides a general framework for understanding ZnO–water–additive interactions in highly filled, peroxide-crosslinked elastomeric systems and offers insights applicable to industrial cable formulations.

2. Materials and Methods

2.1. Materials

EPDM, with a Mooney Viscosity ML (1 + 4) of 60 MU @125 °C, a Propylene content of 27 wt% and an Ethylidene Norbornene content of 4.4 wt%, was purchased from Versalis (San Donato Milanese, Italy). EPM rubber, with a Mooney Viscosity ML (1 + 4) of 40 MU @100 °C and a Propylene content of 48 wt%, was purchased from KUMHO POLY-CHEM (Seoul, Korea). A POE, with an MFI = 1 g/10 min at 190 °C—2.16 kg and a density of 0.885 g/cm^3 was purchased from SABIC (Riyadh, Kingdom of Saudi Arabia). A calcined kaolin clay (Kaolin), with a specific gravity of 2.6 g/cm^3, D50 of 2 µm and a BET of 9 m^2/g was supplied by Imerys (Paris, France). Precipitated ATH, with a density of 2.6 g/cm^3, D50 of 2 µm and a BET of 4 m^2/g was obtained from Huber (Munich, Germany). White ZnO powder with a purity level higher than 99% and BET of 5 m^2/g was bought from Norzinco (Goslar, Germany). Di(tert-butylperoxyisopropyl) benzene (Initiator), as organic peroxide, was purchased from Nouryon (Amsterdam, The Netherlands). AN01, a proprietary concentrate ethylene vinyl acetate (EVA) blend based on 2′,3-bis[[3-(3,5-di-tert-butyl-4-hydroxyphenyl)propionyl]]propionohydrazide, a metal deactivator (MD) and primary phenolic antioxidant, was purchased from Addivant (Danbury, CT, USA), and triallyl cyanurate (TAC) from Kettlitz (Rennertshofen, Germany). AN48, a 70 wt% concentrate of methylmercaptobenzimidazole, was purchased from Lanxess (Cologne, Germany). AN54, a proprietary concentrate blend based on zinc borate, was purchased from SCL (Bergamo, Italy), and synthetic hydrotalcite from Kysuma (Arnhem, the Netherlands).

All the raw materials were used as received, without any purification or modification.

2.2. Compound Preparation

The polymers, together with all other ingredients except for the organic peroxide (excluded to prevent premature crosslinking or scorch), were initially compounded in a 6 L laboratory Banbury mixer (Werner & Pfleiderer, Dinkelsbühl, Germany) equipped with tangential rotors. The mixer consists of a closed chamber with two counter-rotating rotors, providing intensive shear and compressive forces to ensure effective mixing.

The mixing process was carried out at a rotor speed of 60 rpm, following a sequential loading procedure: the polymeric matrix (EPM, EPDM, and POE) was first introduced and masticated for approximately 1 min, followed by the gradual addition of the inorganic filler and minor additives over the next 2–3 min. The total mixing time was approximately 6–7 min, and the compounds were discharged once a temperature of 160 °C was reached, ensuring optimal dispersion and homogenization of the additives and promoting strong interactions between the polymer matrix and the inorganic filler.

The resulting compounds were subsequently transferred to a two-roll mill maintained at 120 °C (G3 S.r.l., Ancarano (TE), Italy). The material was processed for approximately 3–4 min, during which the organic peroxide was added and rapidly incorporated to ensure uniform dispersion within the matrix while minimizing the risk of premature curing. This step also contributes to proper distribution and orientation of the polymer chains.

Finally, the compounds were crosslinked by compression molding in a vertical press (Gibitre Instruments S.r.l., Bergamo, Italy) at 180 °C under a pressure of 25 bar for 5 min, followed by cooling under pressure to room temperature to avoid internal stresses. This process yielded cured plates with a thickness of approximately 1.5 mm.

2.3. Measurements of Resistivity

The volume resistivity (ρ_V) of the samples was measured in accordance with ASTM D257 using a B2985A Electrometer/High Resistance Meter coupled with a 16008B Resistivity Cell (Keysight Technologies, Santa Rosa, California, USA), based on the three-electrode configuration (high voltage electrode, low voltage electrode, and guard electrode).

Prior to testing, all samples were conditioned at 25 °C for 24 h to ensure stabilization of their properties. Measurements were carried out at 25 °C and 100 °C under both dry and wet conditions.

For measurements at 100 °C in air, the samples were thermally conditioned in a calibrated oven (Nabertherm GmbH, Lilienthal, Germany) at 100 °C for 3 h before testing. For measurements in water at 100 °C, the samples were immersed in a thermostatically controlled water bath (laboratory equipment) at 100 °C for 3 h, then removed, surface-dried, and immediately tested.

A DC voltage of 500 V was applied, and resistivity values were recorded after 60 s of electrification, as specified by the standard. Each reported value represents the average of at least three independent measurements performed on different specimens.

3. Results

Industrial mixtures, commonly employed in cable manufacturing, share the same base composition, consisting of EPM, EPDM, and POE as the polymeric matrix, ATH as the main flame-retardant filler, and a fixed amount of minor additives.

At 100 °C, the compound without ZnO shows a ρ_V of 35.7 $\times$ 10^{12} Ω·cm in dry conditions, which decreases to 0.25 $\times$ 10^{12} Ω·cm under wet conditions. The addition of 1.0 phr ZnO slightly increases ρ_V in dry conditions (38.0 $\times$ 10^{12} Ω·cm) and markedly improves the wet resistivity (2.0 $\times$ 10^{12} Ω·cm). At 2.0 phr ZnO, a strong enhancement of dry ρ_V is observed (134.0 $\times$ 10^{12} Ω·cm), while the wet value remains nearly unchanged (1.93 $\times$ 10^{12} Ω·cm).

To better understand the specific role of ZnO in enhancing the insulating properties of the polymer compounds and to isolate the complex interactions involved, simplified formulations were developed. These formulations excluded minor additives, such as antioxidants, plasticizers, and peroxide curing co-activators, in order to focus solely on the interactions between ZnO, the polymer matrix, and the primary filler. Four model compounds consisting only of the polymer matrix, peroxide, and an inorganic filler (either ATH or kaolin), with and without ZnO were prepared and characterized. The detailed compositions of these formulations are presented in Table 1; the components common to all formulations, polymers, flame retardant and the initiator, are reported as weight percent, totaling 100, while the additional components are expressed in phr.

Table 1. Composition and properties of the prepared model compounds.

		Model Compounds			
Components	**Unit**	**ATH-1**	**ATH-2**	**Kaolin-1**	**Kaolin-2**
EPM	wt%	18.0	18.0	18.0	18.0
EPDM	wt%	9.5	9.5	9.5	9.5
POE	wt%	15.4	15.4	15.4	15.4
Initiator	wt%	0.7	0.7	0.7	0.7
ATH	wt%	56.4	56.4	—	—
Kaolin	wt%	—	—	56.4	56.4
ZnO	phr	—	5.0	—	5.0
Properties					
Hardness	Shore A	84.5 ± 0.5	84.5 ± 0.5	86.0 ± 2.0	87.0 ± 1.5
Mooney viscosity	MU	93 ± 3	87 ± 4	113 ± 5	104 ± 6
Tensile strength at break	MPa	12.8 ± 2.3	11.8 ± 2.2	18.1 ± 2.5	17.8 ± 1.8
Elongation at break	%	280 ± 10	281 ± 15	130 ± 18	133 ± 14

Although calcined kaolin is rarely used in flame-retardant cable insulation due to its poor flame-retardant performance, kaolin-based compounds (with and without ZnO) were included in this study to assess the influence of water on insulation performance. Calcined kaolin typically contains less than 2.0 wt% total free moisture, and usually below 0.5 wt% even in high-humidity environments. In contrast, ATH is more hygroscopic and can absorb up to 5–7 wt% water if not adequately protected.

A comparison of the properties reported in Table 1 highlights that the observed differences are primarily governed by the nature of the inorganic filler rather than by the presence of ZnO. In fact, the addition of ZnO does not produce significant variations in hardness, Mooney viscosity, tensile strength, or elongation at break within the same filler system, indicating that it does not substantially affect the crosslinking process or the bulk mechanical behavior of the compounds. In contrast, marked differences are observed when comparing ATH- and kaolin-based formulations. Kaolin-filled compounds exhibit higher hardness and significantly higher Mooney viscosity, which can be attributed to the platelet-like morphology and higher structure of kaolin, leading to stronger filler–polymer interactions and increased resistance to flow during processing. Moreover, kaolin-based systems show higher tensile strength but lower elongation at break compared to ATH-based ones, suggesting a stiffer and more reinforcing behavior. Conversely, ATH, characterized by a more isotropic particle shape and lower reinforcing effect, leads to compounds with lower viscosity, lower stiffness, and higher deformability. These results confirm that, while ZnO has a negligible impact on the bulk physico-mechanical properties, the type of filler plays a dominant role in determining the overall mechanical and rheological behavior of the compounds. Furthermore, SEM observations were performed on selected samples, both before and after water conditioning at 100 °C. No significant differences in particle dispersion or microstructure were observed (Figure S1). These results indicate that the variations in electrical resistivity cannot be attributed to morphological changes in the compound.

Under dry conditions at 100 °C, the ρ_V of the ATH-based compounds without ZnO was nearly three times higher than that of the corresponding kaolin-based compounds. The ZnO-containing compounds show significantly lower resistivity for ATH, whereas the resistivity of kaolin-based formulations is substantially constant.

Under wet conditions at high temperature, the resistivity was drastically reduced for all samples examined, with a significant larger reduction in case of the samples containing ATH. Indeed, while in ATH-based compounds the drop was about one order of magnitude, for the kaolin-based compounds the resistivity decrease was about 50%. Under wet conditions, kaolin-filled compounds show higher resistivity than the analogous ATH-filled ones, although both remain below the required limit (Figure 1). For the ZnO-containing samples, the kaolin–ATH difference does not increase: the values are comparable within the experimental error. The experimental trends observed in Figure 1, where ATH-based compounds exhibit a more pronounced drop in resistivity under wet conditions compared to kaolin-based systems, confirm the dominant role of filler hygroscopicity in controlling electrical performance. To further investigate the system, additional compounds were then prepared starting with the same polymer matrix and base components, but incorporating additional additives, which were not present in the simplified systems described in Table 2. The new formulations were prepared both with and without ZnO, and with various additives introduced either individually or jointly. The used additives are commercial and are pre-dispersed concentrates (masterbatch), including AN01, consisting of triallyl cyanurate (TAC), a crosslinking coagent, and a primary phenolic antioxidant and metal deactivator (MD) dispersed in EVA; AN48, consisting of MMBI, a secondary antioxidant (hydroperoxide scavenger and effective in protecting the compound from metal poisoning); and AN54, consisting of titanium dioxide, hydrotalcite, and zinc borate dispersed in LDPE. The prepared compositions are listed in Table 2.

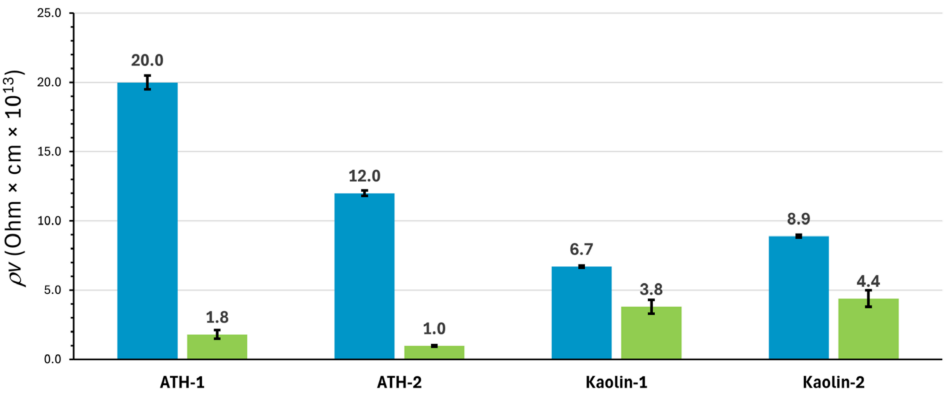


Figure 1. Prepared model compound resistivity under dry (blue) and wet (green) conditions at 100 °C. Error bars represent ±1 standard deviation (n = 3).

The following graphs and discussion pertain to wet conditions, which are of greater relevance to the objectives of this study and to the intended application of the materials. In dry conditions, the trends follow a similar pattern, but the values are always higher.

The measured resistivity of ATH and kaolin-based samples is shown in Figure 2. These results suggest that the dominant effect associated with the different hygroscopicity of the main fillers is maintained across all formulations, even in the presence of additional additives, which contribute to electrical conductivity to a significant yet secondary extent. In ATH-based compounds, the presence of ZnO alone (sample ATH-O*) or of any individual additive (samples ATH-A, ATH-B, and ATH-D) results in a lower ρ_V compared to ATH-0, which contains no additives. A reduction in ρ_V is also observed when combinations of additives are used, such as AN01 + AN48 (sample ATH-C) and AN01 + AN48 + AN54

(sample ATH-E). Notably, the greatest recovery in ρ_V due to ZnO is observed when AN01 is present—either alone or in combination with AN48 or with all three additives together (AN01 + AN48 + AN54). In contrast, when AN48 or AN54 are present without AN01, the positive effect of ZnO on ρ_V is minimal. When kaolin replaces ATH as the filler, ρ_V under wet conditions at high temperature is generally higher. As with the ATH-based systems, all additives—except ZnO—tend to reduce ρ_V. ZnO alone results in the same resistivity compared to the neat kaolin compound. A recovery in ρ_V is observed with the addition of ZnO when AN01 alone is present (samples Kaolin-A and Kaolin-A*). However, when AN48 or AN54 are added individually, the subsequent addition of ZnO causes a slight decrease in ρ_V. When AN01 is combined with AN48 (sample Kaolin-C), a notable reduction in ρ_V is observed compared to neat kaolin, but the addition of ZnO (sample Kaolin-C*) enables a significant recovery of resistivity. In the case where all three additives are present together (AN01 + AN48 + AN54), the ρ_V drops to a very low level, and the presence of ZnO has no measurable effect.

Table 2. Prepared compounds with ATH or kaolin and various content of minor additives.

PREPARED COMPOUND [1]	AN01	AN48	AN54	ZnO
	phr			
ATH-0 or Kaolin-0	//	//	//	//
ATH-0* or Kaolin-0*	//	//	//	5
ATH-A or Kaolin-A	2.0	//	//	//
ATH-A* or Kaolin-A*	2.0	//	//	5
ATH-B or Kaolin-B	//	0.5	//	//
ATH-B* or Kaolin-B*	//	0.5	//	5
ATH-C or Kaolin-C	2.0	0.5	//	//
ATH-C* or Kaolin-C*	2.0	0.5	//	5
ATH-D or Kaolin-D	//	//	2.5	//
ATH-D* or Kaolin-D*	//	//	2.5	5
ATH-E or Kaolin-E	2.0	0.5	2.5	//
ATH-E* or Kaolin-E*	2.0	0.5	2.5	5

[1] Common components: EPM 18% wt, EPDM 9.5% wt, POE 15.4% wt, ATH or kaolin 56.4% wt, Initiator 0.7% wt. * indicates formulation with ZnO

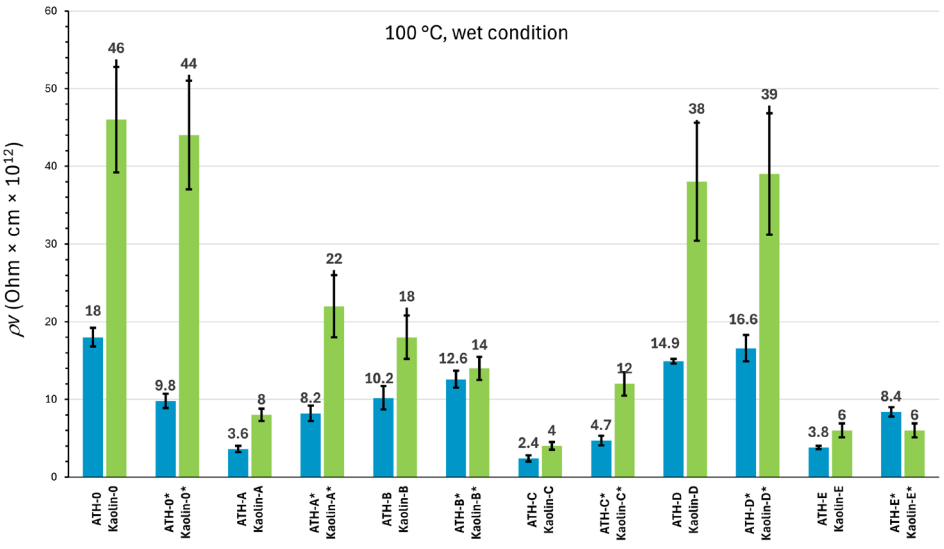


Figure 2. Resistivity of new sample compounds based on ATH (blue) and kaolin (green) with different additives. Error bars represent ±1 standard deviation (n = 3). * indicates formulation with ZnO.

As already mentioned, AN01 is a masterbatch composed of TAC, EVA, and a metal deactivator (MD). To identify which of these components is responsible for the observed interaction with ZnO, simplified compounds were prepared containing only TAC or EVA, both with and without ZnO. These formulations were tested for ρ_V under wet condi-

tions at 100 °C. No variation in resistivity was observed with the addition of ZnO in these systems, suggesting that MD is the component interacting with ZnO to influence electrical properties.

A further series of five kaolin-based compounds were then formulated with a constant concentration of MD (equivalent to that in AN01) and increasing concentrations of ZnO (Table 3,) with kaolin (56.4% wt) chosen as the filler. The selected ZnO concentrations were designed to systematically vary the ZnO/MD ratio, in order to explore its influence on electrical resistivity and identify a possible optimal condition.

Table 3. Kaolin–AN01 mix at different ZnO/MD weight ratios *.

Item	KAO-1	KAO-2	KAO-3	KAO-4	KAO-5
			phr		
MD	0.5	0.5	0.5	0.5	0.5
ZnO	//	1.1	2.6	3.6	5.0

* All complemented by polymer mixture and initiator.

The ρ_V results in wet and dry conditions at 100 °C, shown in Figure 3, confirm that ZnO can partially compensate for the decrease in ρ_V caused by the presence of MD.

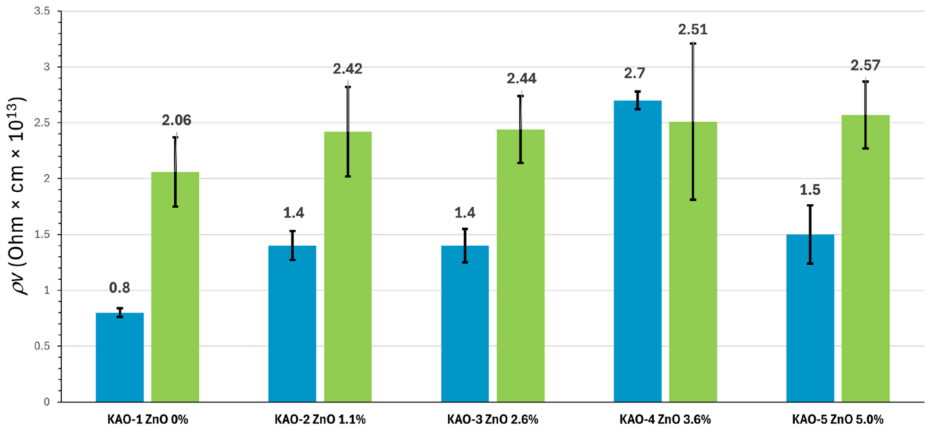


Figure 3. Resistivity of ZnO–AN01 mix at different ZnO/MD weight ratios in dry (green) and wet (blue) conditions, 100 °C. Error bars represent ±1 standard deviation (n = 3).

In dry conditions, increasing the ZnO content results in no significant recovery of resistivity. This behavior is consistent with the mechanism discussed below, as in dry conditions the absence of MD dissociation prevents any beneficial effect of ZnO on resistivity. In wet conditions the extent of this compensating effect is dependent on the ZnO/MD weight ratio. A statistical analysis (based on triplicate measurements) indicates that the increase in resistivity observed for KAO-4 is statistically significant compared to all other formulations ($p < 0.05$). In contrast, no statistically significant differences are observed among KAO-2, KAO-3, and KAO-5, indicating a plateau region. The difference between KAO-1 and intermediate formulations is also statistically significant. Under dry conditions, no statistically significant differences in resistivity are observed among the investigated formulations, as all variations fall within experimental uncertainty. This confirms that the effect of ZnO is not intrinsically related to the polymer matrix but emerges specifically under wet conditions.

4. Discussion

To clarify the role of ZnO in preserving the electrical insulation properties of polymer compounds under wet conditions, a systematic investigation was carried out. By analysing

the influence of individual additives and their interactions with ZnO—particularly the MD—key insights were obtained into the mechanisms governing resistivity stability.

The experimental results on the insulating behavior of the prepared compounds under various conditions indicate that the addition of ZnO negatively impacts the electrical insulating properties, both under dry and wet conditions. This contrasts with the behavior observed in commercial formulations, which contain numerous additional components. Furthermore, the absence of detectable morphological changes (Figure S1), before and after water soaking at high temperature, both in the absence and in the presence of ZnO, supports the hypothesis that the observed variations in resistivity are governed by interfacial or chemical interactions rather than by changes in filler dispersion. Consequently, it can be hypothesized that the positive effects seen in commercial blends arise from interactions between ZnO and one or more of the minor additives.

Formulating a comprehensive mechanistic explanation for the role of ZnO in commercial mixtures is challenging due to the complexity of the formulations and the diversity of molecular species present and due to the possibility that different molecules contribute in opposite ways to the quantitative values of ρ_V. Nonetheless, a general trend emerges: a consistently positive effect of ZnO on resistivity is observed when the complex additive AN01 is included in the compound, as shown in Figure 2 with reference to the ATH-A/ATH-A*, ATH-C/ATH-C* and ATH-E/ATH-E* compounds.

As already mentioned, AN01 is a masterbatch composed of TAC, EVA and a metal deactivator MD. As previously noted, simplified formulations containing only TAC or EVA—with and without ZnO—showed no change in ρ_V under wet conditions, indicating that the metal deactivator (MD) is the key component interacting with ZnO to affect electrical properties.

Also, resistivity measurements of kaolin-based compounds (Figure 3), containing a fixed amount of MD and increasing concentrations of ZnO, confirmed that this can partially offset the reduction in ρ_V caused by MD.

The obtained results indicate that MD and ZnO alone cause a decrease in resistivity under wet conditions. However, when combined, this negative effect is reduced. The extent of recovery appears to depend on achieving an optimal ZnO-to-MD ratio, which may correspond to the amount of MD required to fully coat the surface of the ZnO particles. If this ratio is exceeded, uncoated ZnO particles could contribute to increased electrical conductivity, whereas an insufficient amount of ZnO would leave excess MD unbound and available for dissociation in water [21], thereby compromising insulation [22].

Literature reports support the strong adsorption of phenolic compounds onto ZnO surfaces through hydrogen bonding and electrostatic interactions, even when embedded in a polymer matrix [21]. This phenomenon, well-documented experimentally and theoretically for simple phenol molecules, involves the formation of a monolayer on the ZnO surface [11]. In the case of MD, its bulkier tert-butyl groups introduce steric hindrance, potentially reducing its interaction with the ZnO surface compared to smaller phenolic molecules. Nevertheless, ZnO may still adsorb the hydrazine derivative via its hydroxyl groups, and its nitrogen atoms may act as coordination sites due to their affinity for metal atoms [13]. Based on findings by Karlsson et al., it is presumed that MD-coated ZnO is less conductive than uncoated ZnO [14].

The plausibility of this immobilization mechanism was assessed through an order-of-magnitude estimate of the adsorption capacities of kaolin and ZnO towards MD, based on literature values for specific surface areas and molecular footprints of phenolic compounds on oxide surfaces (see Appendix A, Figure A1 for a schematic representation). The calculations, though based on simplified assumptions, indicate that the combined adsorption capacity of kaolin and ZnO is of the same order of magnitude as the total MD present

in the compound, rendering the proposed mechanism physically plausible. Within this framework, the non-monotonic trend observed in Figure 3—with resistivity increasing from KAO-1 to KAO-4 and then decreasing in KAO-5—is qualitatively consistent with the existence of an optimal ZnO/MD ratio. At low ZnO loadings, the incremental adsorption sites progressively reduce the fraction of MD free to dissociate in water, thereby improving resistivity. At excess ZnO (KAO-5), the uncoated ZnO surface fraction may itself contribute to charge transport under wet conditions, counteracting the benefit. The experimental data thus support the proposed interaction mechanism, while its precise quantitative description requires direct measurement of the relevant adsorption parameters.

The proposed adsorption mechanism is supported by literature evidence on the strong affinity of phenolic compounds for ZnO surfaces [11,21] and on the conductivity-reducing effect of surface coatings on ZnO particles [14]. The interaction of MD with ZnO via its hydroxyl and nitrogen coordination sites is further consistent with known adsorption chemistry of hydrazide derivatives on metal oxide surfaces [13]. Although the actual adsorption behavior of MD, a bulkier molecule than simple phenols, may quantitatively differ and merits future investigation by spectroscopic or computational means, the overall picture is physically well-grounded. Taken together, the experimental results and the supporting mechanistic hypothesis identify the ZnO/MD ratio as a key formulation parameter for achieving stable electrical insulation under hot–wet service conditions, and provide a practical basis for optimizing peroxide-crosslinked elastomeric cable compounds. Additional validation at cable level, using commercial-scale compounds with ZnO/MD ratios representative of the KAO series, confirmed the same non-monotonic trend, with maximum resistivity observed near the optimal composition and reduced performance outside this range.

5. Conclusions

This work investigated the role of zinc oxide in controlling the electrical resistivity of complex flame-retardant elastomeric cable compounds under hot–wet conditions. A stepwise experimental approach allowed the identification of the key interactions governing electrical behavior.

The results show that ZnO does not intrinsically improve the insulation properties of simplified systems and has a negligible effect on bulk physico-mechanical properties. Its beneficial effect emerges only in complex formulations and under wet conditions, where interactions with specific additives become relevant. In particular, the metal deactivator (MD) was identified as the main species responsible for the ZnO-related resistivity recovery.

The resistivity was found to depend strongly on the ZnO/MD ratio, with a non-monotonic trend and an optimal range under wet conditions. This behavior is consistent with a mechanism in which ZnO adsorbs MD, limiting its contribution to ionic conduction in the presence of water. In dry conditions, this mechanism is inactive and no significant effect is observed.

Order-of-magnitude adsorption estimates support the physical plausibility of the proposed mechanism, although they should be regarded as qualitative rather than quantitative.

Overall, the results highlight the dominant role of filler hygroscopicity and the secondary, yet significant, contribution of additive interactions. The identification of an optimal ZnO/MD ratio provides a practical guideline for formulation design aimed at improving insulation performance under service conditions.

Supplementary Materials: The following supporting information can be downloaded at https://www.mdpi.com/article/10.3390/compounds6020028/s1, Figure S1: SEM micrographs of cryogenic fracture of selected compounds with and without ZnO, before and after water conditioning at 100 °C.

Author Contributions: Conceptualization, S.B., F.B. and F.C.; methodology, S.D. and P.M.; validation, A.G.; formal analysis, S.D. and P.M.; investigation, S.D. and P.M.; resources, S.B. and S.D.; data curation, S.B., A.G. and F.B.; writing—original draft preparation, S.B. and F.B.; writing—review and editing, F.C., F.B., S.B. and S.D.; visualization, S.D. and A.G.; supervision, S.B. and F.C.; project administration, S.B. and F.B. All authors have read and agreed to the published version of the manuscript.

Funding: This research received no external funding.

Data Availability Statement: The original contributions presented in this study are included in the article/Supplementary Materials. Further inquiries can be directed to the corresponding author.

Acknowledgments: The authors would like to thank Maria-Beatrice Coltelli for the fruitful discussions. Use of Generative AI: During the preparation of this manuscript, the authors used OpenAI ChatGPT (GPT-5.3) to assist in rephrasing and improving the clarity and fluency of the English text. All scientific concepts, interpretations, and conclusions were entirely provided by the authors. The authors have reviewed and edited the output and take full responsibility for the content of this publication.

Conflicts of Interest: Sabrina Bianchi, Flavia Bartoli and Francesco Ciardelli were employed by the company SPINPET S.r.l.; Stefano Dossi, Andrea Galanti and Pietro Matteucci were employed by the company MIXER S.p.A. The remaining authors declare that the research was conducted in the absence of any commercial or financial relationships that could be construed as a potential conflict of interest.

Abbreviations

The following abbreviations are used in this manuscript:

EPM	Ethylene–Propylene Monomer
EPDM	Ethylene–Propylene–Diene Monomer
POE	Polyolefin Elastomer
EVA	Ethylene–Vinyl Acetate
ATH	Aluminium Trihydroxide
ZnO	Zinc Oxide
MD	Metal Deactivator
TAC	Triallyl Cyanurate
MMBI	Methylmercaptobenzimidazole
HALS	Hindered Amine Light Stabilizer
LDPE	Low-Density Polyethylene
ρ_V	Volume Resistivity
phr	Parts per Hundred Rubber
MU	Mooney Units
MFI	Melt Flow Index
BET	Brunauer–Emmett–Teller
SSA	Specific Surface Area

Appendix A. Order-of-Magnitude Plausibility Check for the MD–ZnO Adsorption Mechanism

The estimates presented in this appendix are intended as a plausibility assessment rather than a quantitative prediction. Their purpose is to verify that the amounts of MD present in the compound are compatible in order of magnitude with the combined adsorption capacity of the inorganic fillers, thereby supporting the physical consistency of the proposed immobilization mechanism. The assumed parameters are acknowledged to carry significant uncertainty, and the results should be interpreted accordingly; direct experimental validation via adsorption isotherms or spectroscopic characterization is recommended in future work.

It is also relevant to consider that phenol is known to adsorb onto metakaolin [23,24], which is present in significantly larger quantities (56.4 g per 100 g of compound) than ZnO. The maximum adsorption capacity (q_{max}) of kaolin towards MD is approximated from the specific surface area (SSA) of kaolin and the molecular footprint of MD, by relating the total available surface area to the area occupied by a single MD molecule accounting for the density of active adsorption sites:

$$q_{max} = N_A \times S \times \theta/(A_m \times 10^{18}) \times M_{MD} \quad (A1)$$

where N_A is Avogadro's number, S is the kaolin specific surface area (m^2/g), θ is the fraction of available active sites, A_m is the molecular cross-sectional area of MD (nm^2), and M_{MD} is the molar mass of MD. In polymer–metakaolin composites, the accessibility of adsorption sites may be reduced by polymer coverage. An effective adsorption capacity ($q_{max,eff}$) is therefore defined as:

$$q_{max,eff} = f_a \times q_{max} \quad (A2)$$

where $0 < f_a \leq 1$ reflects the fraction of kaolin surface accessible to MD molecules within the polymer matrix. The parameter values used in this calculation are summarized in Table A1. The assumptions underlying these parameters are based on literature values and simplified geometrical considerations. In particular, the effective surface area accounts for partial filler disaggregation during melt mixing, the molecular footprint of MD is estimated by scaling from phenol due to its similar functional groups, and an accessibility factor is introduced to account for the fraction of filler surface effectively available within the polymer matrix. These approximations are intended to provide a physically reasonable estimate of adsorption capacity rather than an exact quantitative description. A surface area of 90 m^2/g is assumed for kaolin (ten times the raw BET value of 9 m^2/g), reflecting partial disaggregation of particles during melt mixing [25,26]. The molecular cross-sectional area of MD is estimated at 2 nm^2, based on the known footprint of phenol (~0.4 nm^2), which is used here as a reference molecule due to its well-documented adsorption on ZnO surfaces, and the substantially larger and sterically hindered structure of MD [11]. The degree of coverage θ is set to 0.5 [27], and an accessibility factor $f_a = 0.4$ is applied as a conservative lower bound. A schematic illustration of the adsorption geometry is shown in Figure A1.

Table A1. Estimated parameter value for $q_{max,eff}$ of MD absorption onto kaolin.

Parameters	Explanation	Value
S	kaolin specific surface area (m^2/g)	90
θ	fraction of available active sites	0.5
A_m	molecular cross-sectional area of MD (nm^2)	2
M_{MD}	MD molar mass	553
f_a	accessibility factor	0.4

Using the value based on the previous assumptions, summarized in Table A1 and using Equation (A1) and Equation (A2), the amount of MD that can be absorbed by the amount of kaolin present in KAO-1 to KAO-5 was calculated, resulting in 466 mg.

For ZnO, an adsorption capacity of approximately 12 mg of MD per gram of ZnO has been reported for particles similar in size to those used in this study [10].

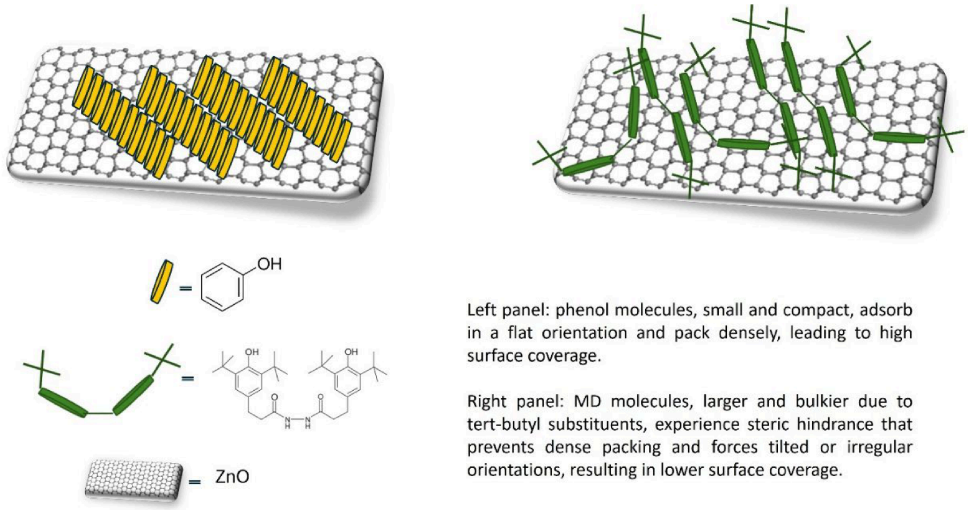


Figure A1. Schematic comparison of phenol and MD adsorption on the ZnO surface.

Therefore, the total adsorption capacity of kaolin and ZnO in the different compounds can be calculated (Table A2).

Table A2. Total absorbable MD in different kaolin-based compounds.

	MD Absorbable onto ZnO (mg)	Total Absorbable MD [1] (mg)
KAO-1	//	466
KAO-2	13	479
KAO-3	31	497
KAO-4	43	509
KAO-5	54	520

[1] considering 466 mg of MD absorbed onto Kaolin.

The estimates reported in Table A2 are intended as an order-of-magnitude plausibility assessment rather than a quantitative prediction. Given the inherent uncertainty in the assumed parameters—particularly the effective surface area of kaolin after melt mixing and the molecular footprint of MD on oxide surfaces—the absolute values of total adsorbable MD should be treated with caution. Nonetheless, the estimates indicate that the combined adsorption capacity of kaolin and ZnO is of the same order of magnitude as the total MD present in the compound, rendering the proposed immobilization mechanism physically plausible. Within this framework, the non-monotonic trend observed in Figure 3—with resistivity increasing from KAO-1 to KAO-4 and then decreasing in KAO-5—is qualitatively consistent with the existence of an optimal ZnO/MD ratio. At low ZnO loadings, the incremental adsorption sites provided by ZnO progressively reduce the fraction of MD free to dissociate into water, improving resistivity. At excess ZnO (KAO-5), the uncoated fraction of ZnO surface may itself contribute to charge transport under wet conditions, counteracting the benefit. The experimental data thus support the proposed interaction mechanism, while its precise quantitative description requires direct measurement of the relevant adsorption parameters.

References

1. Pleşa, I.; Noţingher, P.V.; Schlögl, S.; Sumereder, C.; Muhr, M. Properties of polymer composites used in high-voltage applications. *Polymers* **2016**, *8*, 173. [CrossRef]
2. Nazrin, A.; Kuan, T.M.; Mansour, D.-E.A.; Farade, R.A.; Mohd Ariffin, A.; Abd Rahman, M.S.; Abdul Wahab, N.I. Innovative approaches for augmenting dielectric properties in cross-linked polyethylene (XLPE): A review. *Heliyon* **2024**, *10*, e34737. [CrossRef] [PubMed]

3. Angalane, S.K.; Kasinathan, E. A review on polymeric insulation for high-voltage application under various stress conditions. *Polym. Compos.* **2022**, *43*, 4803–4834. [CrossRef]
4. Tsianakas, V.; Danikas, M.G.; Sarathi, R.; Falekas, G. Applications of polymer nanocomposites in high voltage engineering: A Concise Review on Possible Applications and Questions Regarding Some Limitations. *J. Eng. Sci. Technol. Rev.* **2023**, *16*, 156–163. [CrossRef]
5. Pan, X.; Wang, Z.; Zhou, W.; Liu, F.; Chen, J. Research Progress on Polymer Materials in High-Voltage Applications: A Review. *Energies* **2026**, *19*, 504. [CrossRef]
6. Bouguedad, D.; Mouri, D.; Fofana, I.; Hadjadj, A. Effects of climatic aging on the performance of EPDM used in power cable insulation. In Proceedings of the 2024 IEEE 5th International Conference on Dielectrics (ICD), Toulouse, France, 30 June–4 July 2024. [CrossRef]
7. Liang, B.; Lan, R.; Zang, Q.; Liu, Z.; Tian, L.; Wang, Z.; Li, G. Influence of thermal aging on dielectric properties of high-voltage cable insulation layer. *Coatings* **2023**, *13*, 527. [CrossRef]
8. Liu, W.; Cheng, L.; Li, S. Review of electrical properties for polypropylene-based nanocomposite. *Compos. Commun.* **2018**, *10*, 221–225. [CrossRef]
9. Das, S.K.; Bharatiya, D.; Parhi, B.; Swain, S.K. Influential factors modulating the dielectric behaviour of transition metal oxide nanocomposites for energy storage applications: A state-of-the-art review. *J. Energy Storage* **2023**, *73*, 108930. [CrossRef]
10. Özgür, Ü.; Alivov, Y.I.; Liu, C.; Teke, A.; Reshchikov, M.A.; Doğan, S.; Avrutin, V.; Cho, S.-J.; Morkoç, H. A comprehensive review of ZnO materials and devices. *J. Appl. Phys.* **2005**, *98*, 041301. [CrossRef]
11. Dehmani, Y.; Lainé, J.; Daouli, A.; Sellaoui, L.; Bonilla-Petriciolet, A.; Lamhasni, T.; Abouarnadasse, S.; Badawi, M. Unravelling the adsorption mechanism of phenol on zinc oxide at various coverages via statistical physics, artificial neural network modeling and ab initio molecular dynamics. *Chem. Eng. J.* **2023**, *452*, 139171. [CrossRef]
12. Hong, J.I.; Winberg, P.; Schadler, L.S.; Siegel, R.W. Dielectric properties of zinc oxide/low-density polyethylene nanocomposites. *Mater. Lett.* **2005**, *59*, 473–476. [CrossRef]
13. Kusmierz, M.; Pasieczna-Patkowska, S. FT-IR/PAS study of surface EDTA–ZnO interactions. *Ann. Univ. Mariae Curie-Skłodowska Sect. AA Chem.* **2014**, *68*, 25–31. [CrossRef]
14. Karlsson, M.E.; Calamida, A.; Forchheimer, D.; Hillborg, H.; Ström, V.; Gardner, J.M.; Hedenqvist, M.S.; Olsson, R.T. The effect of ZnO particle lattice termination on the DC conductivity of LDPE nanocomposites. *Mater. Adv.* **2020**, *1*, 1653–1664. [CrossRef]
15. Caramitu, A.R.; Lungu, M.V.; Ciobanu, R.C.; Ion, I.; Lungulescu, E.M.; Sbarcea, G.B.; Marinescu, V.E.; Aradoaei, S.; Aradoaei, M.; Machidon, R. Composites from recycled HDPE and ZnO nanopowder for cable jacketing applications. *Polymers* **2025**, *17*, 1987. [CrossRef]
16. Ullah, W.; Abbas, M.F.; Khan, S.; Flah, A.; El-Bayeh, C.Z.; Shoush, K.A.; Saman, B. Impact of Electro-UV Aging on the Insulation Performance of PVC/ZnO Nanocomposites for Outdoor Applications. *IEEE Access* **2025**, *13*, 67415–67433. [CrossRef]
17. Benabid, F.Z.; Benaceur, H.; AL-Oqla, F.M.; Mallem, O.K. ZnO/LDPENano-composites: Effects of Particle Size and Electrical Resistivity on Mechanical, Electrical, and Thermal Properties: A Review. *Jordan J. Mech. Ind. Eng.* **2024**, *18*, 797–806. [CrossRef]
18. Beißmann, S.; Reisinger, M.; Grabmayer, K.; Wallner, G.; Nitsche, D.; Buchberger, W. Analytical evaluation of the performance of stabilization systems for polyolefinic materials. Part I: Interactions between hindered amine light stabilizers and phenolic antioxidants. *Polym. Degrad. Stab.* **2014**, *110*, 498–508. [CrossRef]
19. Beißmann, S.; Grabmayer, K.; Wallner, G.; Nitsche, D.; Buchberger, W. Analytical evaluation of the performance of stabilization systems for polyolefinic materials. Part II: Interactions between hindered amine light stabilizers and thiosynergists. *Polym. Degrad. Stab.* **2014**, *110*, 509–517. [CrossRef]
20. Liu, D.; Pourrahimi, A.M.; Pallon, L.K.H.; Cobo Sánchez, C.; Olsson, R.T.; Hedenqvist, M.S.; Fogelström, L.; Malmström, E.; Gedde, U.W. Interactions between a phenolic antioxidant, moisture, peroxide and crosslinking by-products with metal oxide nanoparticles in branched polyethylene. *Polym. Degrad. Stab.* **2016**, *125*, 21–32. [CrossRef]
21. Bertoldo, M.; Ciardelli, F. Water extraction and degradation of a sterically hindered phenolic antioxidant in polypropylene films. *Polymer* **2004**, *45*, 8751–8759. [CrossRef]
22. Nilsson, F.; Karlsson, M.; Pallon, L.; Giacinti, M.; Olsson, R.T.; Venturi, D.; Gedde, U.W.; Hedenqvist, M.S. Influence of water uptake on the electrical DC-conductivity of insulating LDPE/MgO nanocomposites. *Compos. Sci. Technol.* **2017**, *152*, 11–19. [CrossRef]
23. Lainé, J.; Foucaud, Y.; Bonilla-Petriciolet, A.; Badawi, M. Molecular picture of the adsorption of phenol, toluene, carbon dioxide and water on kaolinite basal surfaces. *Appl. Surf. Sci.* **2022**, *585*, 152699. [CrossRef]
24. Alkaram, U.F.; Mukhlis, A.A.; Al-Dujaili, A.H. The removal of phenol from aqueous solutions by adsorption using surfactant-modified bentonite and kaolinite. *J. Hazard. Mater.* **2009**, *169*, 324–332. [CrossRef]
25. Taguet, A.; Cassagnau, P.; Lopez-Cuesta, J.-M. Structuration, selective dispersion and compatibilizing effect of (nano)fillers in polymer blends. *Prog. Polym. Sci.* **2014**, *39*, 1526–1563. [CrossRef]

26. Kasaliwal, G.R.; Pegel, S.; Göldel, A.; Pötschke, P.; Gert, H. Analysis of agglomerate dispersion mechanisms of multiwalled carbon nanotubes during melt mixing in polycarbonate. *Polymer* **2010**, *51*, 2708–2720. [CrossRef]
27. Adamson, A.W.; Gast, A.P. *Physical Chemistry of Surfaces*, 6th ed.; Wiley: New York, NY, USA, 1997; Available online: https://www.wiley.com/en-ca/Physical+Chemistry+of+Surfaces%2C+6th+Edition-p-9780471148739 (accessed on 1 March 2026).

Disclaimer/Publisher's Note: The statements, opinions and data contained in all publications are solely those of the individual author(s) and contributor(s) and not of MDPI and/or the editor(s). MDPI and/or the editor(s) disclaim responsibility for any injury to people or property resulting from any ideas, methods, instructions or products referred to in the content.